# Radiometric calibration of multiple Earth observation sensors using airborne hyperspectral data at the Newell County rangeland test site

Philippe M. Teillet [*a], Gunar Fedosejevs [a], Robert P. Gauthier [a], Raymond T. Shin [a], Norman T. O'Neill [b], Kurtis J. Thome [c], Stuart F. Biggar [c], Herbert Ripley [d], and Aimé Meygret [e]

[a] Canada Centre for Remote Sensing, 588 Booth Street, Ottawa, Ontario, Canada K1A 0Y7
[b] CARTEL, Université de Sherbrooke, Sherbrooke, Québec, Canada J1K 2R1
[c] Optical Sciences Center, University of Arizona, Tucson, Arizona, USA 85721-0094
[d] Hyperspectral Data International, One Research Drive, Dartmouth, Nova Scotia, Canada B2Y 4M9
[e] Centre national d'études spatiales, BPI 811, 18, avenue Edouard Bélin, 31401 Toulouse, Cedex 4, France

## ABSTRACT

A single data set of spatially extensive hyperspectral imagery is used to carry out vicarious calibrations for multiple Earth observation sensors. Results are presented based on a data acquisition campaign at the Newell County rangeland test site in Alberta in October 1998, which included ground-based measurements, satellite imagery, and airborne *casi* hyperspectral data. This paper presents new calibration monitoring results obtained for NOAA-14 AVHRR, OrbView-2 SeaWiFS, SPOT-4 VGT, Landsat-5 TM, and SPOT-2 HRV.

**Keywords:** Sensor radiometric calibration; vicarious calibration; test sites; airborne hyperspectral remote sensing.

## 1. INTRODUCTION

Experimental work is being done to test the feasibility of using single hyperspectral data sets to carry out vicarious calibrations for multiple sensors. The domain of interest and applicability is that of optical sensors with spectral bands in the range encompassed by the reference hyperspectral sensor. The approach is applicable to sensors with large footprints (1-km, for example) and small footprints (20-m, for example). Such a capability has the potential to provide timely monitoring of quality assurance and stability reference (QUASAR) test sites for calibration purposes. The first results from this QUASAR monitoring methodology[1,2] used two hyperspectral data sets to generate radiometric calibration estimates for six Earth observation sensors, namely the NOAA-14 Advanced Very High Resolution Radiometer (AVHRR), Orbview-2 Sea-viewing Wide-Field-of-view Sensor (SeaWiFS), SPOT-4 Vegetation (VGT), Landsat-5 Thematic Mapper (TM), and SPOT-1 and SPOT-2 Haute résolution visible (HRV) sensors.

A QUASAR monitoring data acquisition campaign took place at the Newell County rangeland test site in Alberta on October 4, 1998, including ground-based measurements, satellite imagery, and airborne hyperspectral data. The airborne imagery was acquired using the Compact Airborne Spectrographic Imager (*casi*). This paper examines the suitability of the rangeland test site and highlights new radiometric calibration estimates for five Earth observation sensors that all imaged the Newell County test site on 4 October 1998: NOAA-14 AVHRR, OrbView-2 SeaWiFS, SPOT-4 VGT, Landsat-5 TM, and SPOT-2 HRV. New results are also presented for SeaWiFS based on a data acquisition campaign at the Alberta site in August 1998.

[*] Correspondence: Email: phil.teillet@ccrs.nrcan.gc.ca; Telephone: 613 947 1251; Fax: 613 947 1383

## 2. THE QUASAR APPROACH

The QUASAR methodology[1] is briefly summarized as follows. Airborne mission and field measurement methodologies have been created to acquire spatially extensive hyperspectral imagery over selected test sites as well as ground-level ancillary and validation data sets. A data processing and analysis scheme has been formulated and implemented in prototype mode to retrieve an average surface reflectance spectrum for the test site under consideration and to predict top-of-atmosphere (TOA) radiances for satellite sensors of interest for calibration monitoring purposes. The Imaging Spectrometer Data Analysis System (ISDAS)[3] at the Canada Centre for Remote Sensing was used to carry out the atmospheric computations using the Modtran-3 radiative transfer code and a look-up table approach[4]. The accuracy of the QUASAR approach is estimated to be on the order of ± 6 percent (one sigma)[5]. A detailed error budget analysis is in progress[6]. The hyperspectral and spatially extensive nature of such benchmark data sets makes it possible to attempt vicarious calibrations for any sensor(s) with appropriate characteristics that imaged the test site on the same day, or within a day or two if atmospheric and surface conditions have not changed significantly. Appropriate sensors include any with footprints that fit comfortably within the test site and with one or more spectral bands encompassed by the wavelength coverage of the airborne hyperspectral sensor. Spectral bands outside the wavelength range of the reference sensor can be monitored using inter-band relative calibration methods.

## 3. TEST SITES AND DATA SETS

The test site is a 7 km by 7 km area in prairie rangeland in Newell County, Alberta (hereafter referred to as NCRA) located north-west of Medicine Hat, Alberta at 50° 18' N and 111° 38' W and at an elevation of 750 m above sea level. Given its reasonable proximity to urban areas from which hyperspectral sensors can be flown and its lower reflectance compared to desert sites, Newell County rangeland in Alberta has the potential to serve as a routine test site for interim performance monitoring of satellite sensors.[1] The QUASAR approach has also been tested at the Railroad Valley playa in Nevada (RVPN) for a 7 km by 7 km test site. The playa location has a growing history of international use as a test site for vicarious calibration and it serves as a good setting for the QUASAR methodology proof-of-concept. Both test sites are described in greater detail by Teillet et al. [1,7,8]

Radiometric uniformity studies were used to determine the location and size of the primary test sites in the Railroad Valley and Newell County areas.[8] Image data at 1-km spatial scale were simulated from SPOT HRV imagery in order to characterize radiometric uniformity with the calibration of large footprint sensors primarily in mind. For single-date 1-km images of both the RVPN area and the NCRA area, it was found that there are windows 7 km by 7 km in size that have coefficients of variation less than or equal to 3 percent in all three HRV spectral bands. For a selected prime site of 7 km by 7 km at each location, descriptive statistics from the 1-km data indicate that both sites could be equally useful as vicarious calibration sites for large footprint sensors. [8] Radiometric uniformity characteristics of sub-areas within the prime sites at both locations indicate that test site sizes of 5 km by 5 km may have to be considered in the future if greater uniformity is needed. For the images used in the uniformity study, such site dimensions would yield coefficients of variation of 2 percent in all three HRV spectral bands. Test sites 5 km by 5 km in size could preclude the use of pixels at very large off-nadir angles in vicarious calibration schemes. Further data analyses and experience with the test sites should lead to a better understanding of seasonal characteristics, directional reflectance properties, and radiometric uniformity at finer spatial scales.

Data acquisition campaigns took place at the RVPN test site in June 1998 and at the NCRA test site in August 1998 and October 1998, including ground-based measurements, satellite imagery, and airborne hyperspectral data in all cases. For the October NCRA data acquisition campaign of primary interest in this paper, near-coincident satellite sensor imagery was acquired on the *casi* flight day, October 4, 1998, by NOAA-14 AVHRR, OrbView-2 SeaWiFS, SPOT-4 VGT, Landsat-5 TM, and SPOT-2 HRV. Other AVHRR, VGT, and SeaWiFS data were also acquired within a few days of October 4. The airborne *casi* imagery was acquired at a flight altitude of 3000 meters above sea level (2245 meters above ground level) such that the spatial resolution of the data is approximately 3 meters. Eleven parallel flight lines were used to cover the 7 km by 7 km test site. A 100-meter by 100-meter ground validation site within the *casi* data coverage area was selected at the NCRA test site for ground-based measurements. These measurements included GER3700™ spectrometer measurements made over the surface and over a Labsphere Spectralon™ reflectance panel to generate surface reflectances for use in validating surface reflectances retrieved from the *casi* imagery. Despite plans to the contrary, sunphotometer measurements were not available during the October data acquisition campaign. Atmospheric conditions were clear and a standard value of 0.05 was assumed for the atmospheric aerosol optical depth at 0.550 micrometers (AOD550).

## 4. DATA PROCESSING

The main data processing steps are as follows [1]:

1. input hyperspectral flight line image in radiance units;
2. correct flight line image for aircraft roll variations;
3. extract test site coverage segment from flight line image;
4. compute average scan-angle image for flight line image segment;
5. retrieve surface spectral reflectances from average scan-angle image;
6. calculate pixel-averaged surface reflectance spectrum for flight line image segment;
7. repeat above processing steps for all flight lines;
8. obtain average surface reflectance spectrum for test site;
9. adjust surface reflectances to sun/view geometry of selected satellite sensor image acquisition;
10. compute TOA radiance spectrum for selected satellite sensor;
11. integrate TOA radiance spectrum over selected satellite sensor spectral band.

It is assumed that the TOA radiance estimates obtained from the QUASAR methodology (i.e., the output of step 11) for the various satellite sensor spectral bands are representative of the entire 7-km by 7-km test site. Thus, digital signal levels (DSL, in counts) can be extracted from relevant satellite sensor images of the test sites and combined with the TOA radiances to generate QUASAR estimates of radiometric calibration gain coefficients in counts per unit radiance. With a reference area of 7 km by 7 km, it is possible to accommodate several image pixels even for large footprint sensors and still stay well within the boundaries of the area to allow for location errors. For comparison, the nominal post-launch calibration coefficients were obtained from the pertinent sources. For AVHRR, the coefficients are from the NASA Goddard Space Flight Center and based on ocean and cloud scene methodologies.[9] For SeaWiFS, the calibration is obtained by running the SeaWiFS Data Analysis System (SeaDAS) package.[10] For TM, HRV, and VGT, the calibration coefficients were taken from the product tape header and/or the product documentation.

## 5. PREVIOUS RESULTS

### 5.1 RVPN Test Site (June 1998 Campaign)

Based on the RVPN data acquisition campaign in June 1998, initial QUASAR monitoring results were obtained for NOAA-14 AVHRR spectral band 1, OrbView-2 SeaWiFS spectral bands 1 to 8, Landsat-5 TM spectral bands 1 to 4, and SPOT-1 HRV spectral bands 1 to 3 (cf. Teillet et al.[1,2], for details). The main results consist of *casi*-based TOA radiance predictions and their percentage difference comparisons with satellite image-based TOA radiances determined independently using nominal post-launch calibration coefficients (Figure 1). The QUASAR approach predicts a TOA radiance within 5.1 percent of the nominal NOAA-14 AVHRR calibration on the day of the airborne *casi* data acquisition (June 17). Good matches in the range of -2 to -5 percent were also obtained for AVHRR cases on three consecutive days (June 18-20) after the *casi* flight for predominantly forward scattering geometries (Figure 1). QUASAR results for four other AVHRR cases (June 19-22), all with predominantly backward scattering geometries, yielded TOA radiances significantly lower than nominal (differences of –18.3 to –26.2 percent). The reasons for these differences are not yet understood. The QUASAR approach yields TOA radiance estimates for SeaWiFS that are generally in good agreement with nominal values (within 5 percent on average) for both June 17 and 18, but the mismatches approach 10 percent in some spectral bands. For VGT, the QUASAR TOA radiance results are significantly lower than nominal (differences of –8.7 to –16.6 percent). These differences are not yet understood, but they are consistent with AVHRR results found for similar scattering geometries.

Figure 1. Comparison of top-of-atmosphere (TOA) radiance results for the RVPN test site for June 14-22, 1998 and the NCRA test site for August 4-10, 1998. The satellite sensors cases include thirteen NOAA-14 AVHRR cases (spectral band 1), one SPOT-4 VGT case (spectral bands B0, B2, B3), two OrbView-2 SeaWiFS cases (spectral bands 1-8), two Landsat-5 TM cases (spectral bands 1-4), one SPOT-1 HRV case (spectral bands 1-3), and one SPOT-2 HRV case (spectral bands 1-3). The error bars represent ± 6 percent uncertainty levels. The diagonal line is the unity slope line.

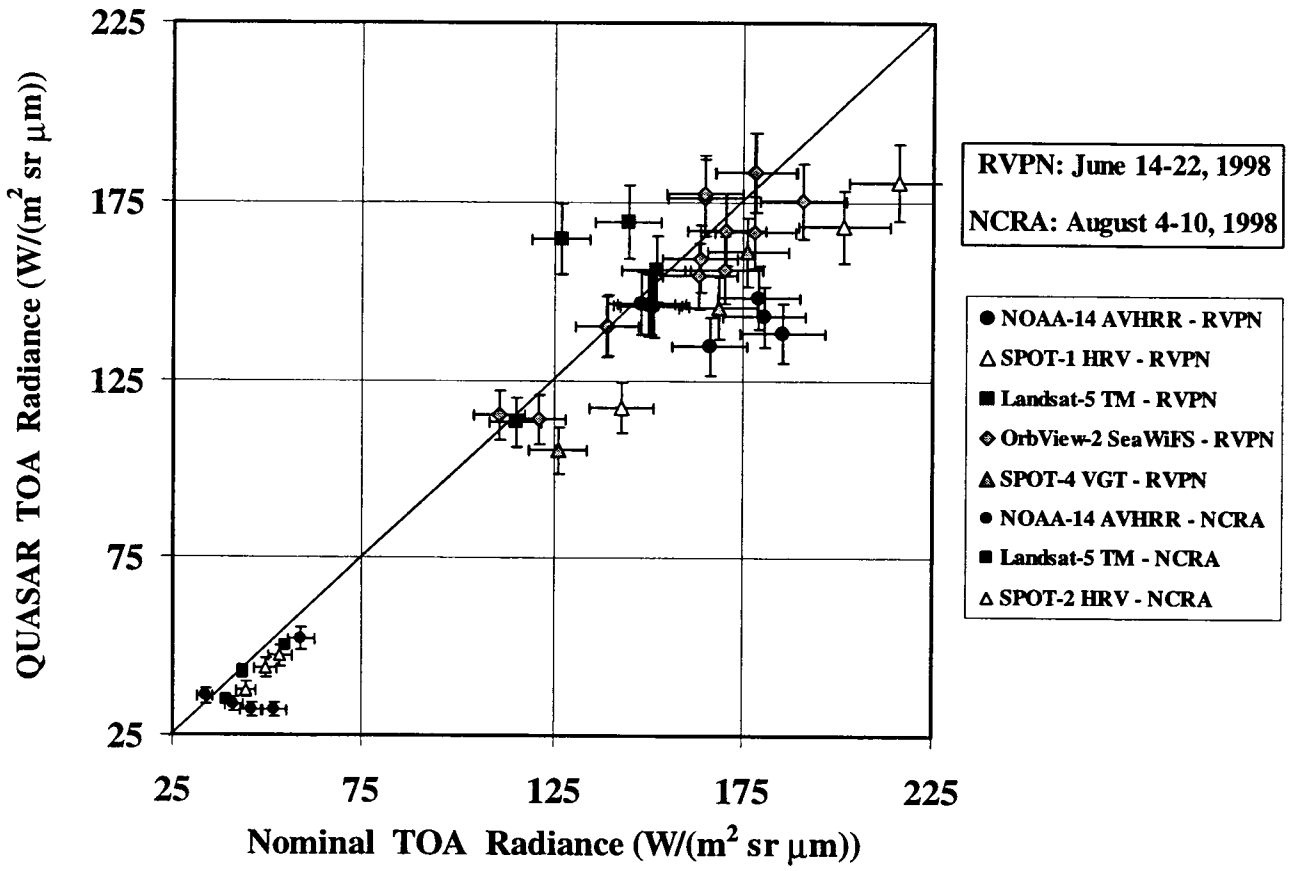


With respect to small footprint sensors, none of the satellite sensor data sets were acquired on the same day as the airborne hyperspectral data acquisition. Therefore, the generation of QUASAR monitoring results in these cases relies exclusively on temporal extrapolations of surface and atmospheric conditions ranging from one to three days. Although good matches in the range of +3 to –2 to percent were obtained for TM spectral bands 3 and 4, the RVPN QUASAR data set does not provide a good reference for Landsat-5 TM spectral bands 1 and 2 three days earlier (June 14) because of changes in the playa surface while it was drying after a rainy period earlier in the month. The days following a wet period should be avoided and/or a better knowledge of the RVPN test site's characteristics as a function of time while drying needs to be developed. The QUASAR results for the SPOT-1 HRV spectral bands predict lower TOA radiances than the nominal radiances (Figure 1) and hence less sensor degradation (i.e., more counts per unit radiance). For the SPOT-1 HRV case, the one-day signature extension (to June 18) is reasonable since visual observations indicated essentially identical surface and atmospheric conditions and the consistency of the RVPN QUASAR results for AVHRR (forward scattering cases) support this assumption.

### 5.2 NCRA Test Site (August 1998 Campaign)

Based on the data acquisition campaign at the NCRA test site in August, 1998, initial QUASAR monitoring results were obtained for NOAA-14 AVHRR spectral band 1, Landsat-5 TM spectral bands 1 to 4, and SPOT-2 HRV spectral bands 1 to 3 (cf. Teillet et al. [1], for details). The main QUASAR result (Figure 1) predicts a TOA radiance within 6.3 percent of the nominal NOAA-14 AVHRR calibration on the day of the airborne *casi* data acquisition (August 4). QUASAR results for four other AVHRR cases on subsequent days (August 6, 8, 9, and 10), all with predominantly backward scattering geometries, yielded TOA radiances significantly lower than nominal (differences of –18.3 to –26.2 percent). Again, the reasons for these differences are not yet understood.

With respect to small footprint sensor coverage, none of the satellite sensor data sets were acquired on the same day as the airborne hyperspectral data acquisitions. For TM data acquired four days after the *casi* data acquisition (August 8), good matches in the range of –1 to –3 percent were obtained for TM spectral bands 2 and 4. QUASAR results for TM spectral bands 1 and 3 predict TOA radiances 8 to 11 percent lower than the radiances based on nominal post-launch calibration. The QUASAR results for SPOT-2 HRV spectral bands predict TOA radiances –11 to –15 percent lower than nominal radiances as well.

### 5.3 Surface Reflectance Comparisons

For comparison and validation purposes, average surface reflectances from atmospherically-corrected *casi* data were compared to GER3700-based surface reflectances obtained by convolution of the average GER spectrum for the 100-meter by 100-meter ground validation site with the relative spectral response profile for the relevant satellite sensor spectral band. For both the June RVPN and August NCRA campaigns, the agreement between the *casi*-based surface reflectances averaged over the 7-km by 7-km test site and those from the GER3700 for the ground validation site is within 10 percent. The agreement between *casi*-based surface reflectances restricted to pixels for the ground validation site and the GER3700-based surface reflectances for the ground validation site is within 5 percent except for TM band 4 and HRV band 3 for the NCRA test site. These are reasonable results given the completely independent data and methods involved.

### 5.4 Main Conclusions of Previous Work

The main conclusions drawn from previous QUASAR results are as follows.

1. An experimental QUASAR monitoring methodology has been developed and tested at the RVPN and NCRA test sites.
2. QUASAR calibration results were generated for multiple cases of six Earth observation sensors from two hyperspectral data acquisition campaigns.
3. Surface reflectances obtained from *casi*-based QUASAR spectra and GER3700-based spectra agree to within 5 percent for all of the satellite sensor spectral bands studied except TM band 4 and HRV band 3 for the NCRA test site.
4. For satellite data acquired on the *casi* flight days, QUASAR calibration results match within uncertainties the nominal post-launch calibration results for NOAA-14 AVHRR and OrbView-2 SeaWiFS, but not for SPOT-4 VGT.
5. Temporal extensions of QUASAR data sets to days near to *casi* data acquisition days yield:
   - good results for OrbView-2 SeaWiFS (RVPN test site);
   - good results for NOAA-14 AVHRR cases with predominantly forward scattering geometries;
   - poor results for NOAA-14 AVHRR cases with predominantly backward scattering geometries;
   - mixed results for Landsat-5 TM cases.
6. There is a systematic offset between QUASAR calibrations and nominal post-launch calibrations for all SPOT sensor cases examined (SPOT-1 HRV, SPOT-2 HRV, and SPOT-4 VGT).
7. The QUASAR methodology requires better knowledge of the bidirectional reflectance characteristics of both the RVPN and NCRA test sites.
8. Preliminary indications are that the NCRA test site is suitable for vicarious calibration.

Table 1. AVHRR and VGT radiometric calibrations based on the NCRA test site for October 1998 [a].

| | *NOAA-14 AVHRR* | *NOAA-14 AVHRR* | *SPOT VGT* | *SPOT VGT* | *SPOT VGT* | *SPOT VGT* | *SPOT VGT* | *SPOT VGT* |
|---|---|---|---|---|---|---|---|---|
| Spectral band | 1 | 1 | B0 | B2 | B3 | B0 | B2 | B3 |
| Central wavelength (μm) | 0.633 | 0.633 | 0.445 | 0.670 | 0.825 | 0.445 | 0.67 | 0.825 |
| Integrated bandpass (μm) | 0.1334 | 0.1334 | 0.0409 | 0.0798 | 0.1198 | 0.0409 | 0.0798 | 0.1198 |
| Exo-atmospheric solar irradiance | 1561.5 | 1561.5 | 1962.5 | 1547.4 | 1047.7 | 1962.5 | 1547.4 | 1047.7 |
| Date | 1998-10-04 | 1998-10-05 | 1998-10-03 | 1998-10-03 | 1998-10-03 | 1998-10-04 | 1998-10-04 | 1998-10-04 |
| Time (UTC) | 21:27 | 21:05 | 18:30 | 18:30 | 18:30 | 18:11 | 18:11 | 18:11 |
| Solar distance (A.U.) | 1.0001 | 0.9998 | 1.0160 | 1.0160 | 1.0160 | 1.0160 | 1.0160 | 1.0160 |
| Solar zenith angle (degrees) | 61.7 | 60.1 | 55.5 | 55.5 | 55.5 | 56.5 | 56.5 | 56.5 |
| Solar azimuth angle (degrees) | 218.0 | 212.1 | 166.5 | 166.5 | 166.5 | 160.5 | 160.5 | 160.5 |
| Satellite zenith angle (degrees) | 12.3 | 36.3 | 13.5 | 13.5 | 13.5 | 35.5 | 35.5 | 35.5 |
| Satellite azimuth angle (degrees) | 77.0 | 77.0 | 108.0 | 108.0 | 108.0 | 100.5 | 100.5 | 100.5 |
| Rayleigh optical depth | 0.0498 | 0.0498 | 0.1752 | 0.0398 | 0.0157 | 0.1752 | 0.0398 | 0.0157 |
| Aerosol optical depth | 0.0419 | 0.0419 | 0.0610 | 0.0404 | 0.0302 | 0.0610 | 0.0404 | 0.0302 |
| Test site RHO from QUASAR (TQ) | 9.6 | 9.6 | 5.3 | 9.9 | 16.7 | 5.3 | 9.9 | 16.7 |
| Val site RHO from GER3700 (G) | 10.3 | 10.3 | 6.2 | 10.5 | 18.4 | 6.2 | 10.5 | 18.4 |
| Δ RHO = % (TQ - G)/G | -6.4% | -6.4% | -14.9% | -5.9% | -9.0% | -14.9% | -5.9% | -9.0% |
| Val site RHO from QUASAR (VQ) | 10.1 | 10.1 | 5.5 | 10.3 | 18.1 | 5.5 | 10.3 | 18.1 |
| Δ RHO = % (VQ - G)/G | -2.1% | -2.1% | -10.7% | -2.1% | -1.4% | -10.7% | -2.1% | -1.4% |
| BRF adjustment factor | 0.88 | 0.77 | 1.11 | 1.11 | 1.11 | 1.45 | 1.45 | 1.45 |
| Image DSL for test site (counts) | 78.06 | 78.72 | | | | | | |
| Test site image RHO* from nominal PLC | | | 14.3 | 12.4 | 18.0 | 17.6 | 14.3 | 20.5 |
| Nominal PLC gain coefficient | 1.4280 | 1.4280 | | | | | | |
| Nominal PLC offset coefficient | 41.000 | 41.000 | | | | | | |
| TOA L* from nominal PLC (N) | 26.0 | 26.4 | 49.1 | 33.5 | 33.0 | 58.6 | 37.6 | 36.5 |
| TOA L* from QUASAR PLC (Q) | 22.9 | 22.7 | 45.8 | 34.2 | 33.4 | 55.3 | 42.3 | 41.5 |
| Δ TOA L* = % (Q - N)/N | -11.8% | -14.1% | -6.8% | 2.0% | 1.3% | -5.7% | 12.5% | 13.7% |

[a] UTC = coordinated universal time; AU = astronomical units; RHO = surface reflectance (%); DSL = digital signal level; BRF = bidirectional reflectance factor; PLC = post-launch calibration; TOA = top of atmosphere; RHO* = TOA reflectance. DSL units are image counts; radiances L* units are W/(m$^2$ sr μm); irradiances units are W/(m$^2$ μm); gain units are counts/radiance. Newell County test site latitude = 50d 18m 20s; longitude = -111d 37m 32s; elevation = 750 m. Ozone content (cm-atm) = 0.319; water vapour content (g/cm$^2$) = 1.35.

## 6. SEAWIFS RESULTS FOR THE AUGUST 1998 CAMPAIGN

Based on the data acquisition campaign at the NCRA test site in August, 1998, QUASAR monitoring results have been generated for OrbView-2 SeaWiFS spectral bands 1 to 8. The predicted TOA radiances in the eight spectral bands are 15 to 30 percent lower than the nominal SeaWiFS radiances on the day of the airborne *casi* data acquisition (August 4). QUASAR results for three other SeaWiFS cases on subsequent days (August 6, 8, and 10) also yield TOA radiances significantly lower than nominal values (differences of –19 to –38 percent). SeaWiFS image acquisition geometries typically have almost orthogonal relative azimuths between the solar and viewing directions and, consequently, bi-directional reflectance effects are not expected to be the main cause of these mismatches.

## 7. RESULTS FOR THE OCTOBER 1998 CAMPAIGN

Multi-sensor radiometric calibration results for the October campaign at the NCRA test site are summarized in Tables 1 to 3. The central wavelengths and integrated bandpasses for the satellite sensor spectral bands are given in the tables. In all cases, the atmospheric parameters pertain to those that were estimated on the *casi* data acquisition date and they are assumed to remain unchanged for the other days. Clearly, this assumption is a potential source of error in the method and, in due course, the trade-off between more data points and reduced accuracy will have to be examined.

Table 2. SeaWiFS radiometric calibrations based on the NCRA test site for October 1998 [a].

| *SeaWiFS spectral band:* | *1* | *2* | *3* | *4* | *5* | *6* | *7* | *8* |
|---|---|---|---|---|---|---|---|---|
| Central wavelength (μm) | 0.412 | 0.443 | 0.490 | 0.510 | 0.555 | 0.67 | 0.765 | 0.865 |
| Integrated bandpass (μm) | 0.0151 | 0.0161 | 0.0173 | 0.0182 | 0.0161 | 0.0167 | 0.0348 | 0.0354 |
| Exo-atmospheric solar irradiance | 1709.47 | 1909.7 | 1932.8 | 1892.3 | 1878.8 | 1536.3 | 1213.7 | 978.1 |
| Rayleigh optical depth | 0.2925 | 0.2129 | 0.1424 | 0.1214 | 0.0860 | 0.0402 | 0.0234 | 0.0142 |
| Aerosol optical depth | 0.0682 | 0.0629 | 0.0568 | 0.0545 | 0.0495 | 0.0397 | 0.0325 | 0.0286 |
| Test site RHO from QUASAR (TQ) | 2.7 | 4.7 | 6.4 | 6.8 | 7.9 | 9.8 | 15.3 | 17.5 |
| Val site RHO from GER3700 (G) | 4.7 | 5.8 | 6.9 | 7.3 | 8.5 | 10.4 | 16.6 | 19.3 |
| Δ RHO = % (TQ - G)/G | -44.1% | -19.7% | -7.1% | -6.8% | -7.8% | -5.9% | -7.8% | -9.5% |
| Val site RHO from QUASAR (VQ) | 2.7 | 4.9 | 6.7 | 7.2 | 8.4 | 10.1 | 17.1 | 18.7 |
| Δ RHO = % (VQ - G)/G | -43.7% | -15.9% | -2.5% | -1.8% | -2.1% | -2.7% | 2.9% | -2.9% |
| *Date = October 4; time (UTC) = 19:45; BRF adjustment factor = 0.83.* | | | | | | | | |
| *Solar distance (A.U.) = 1.0004; solar zenith (deg) = 55.2; solar azimuth (deg) = 189.4; view zenith (deg) = 30.7; view azimuth (deg) = 103.1.* | | | | | | | | |
| Image DSL for test site (counts) | 482.10 | 487.80 | 555.80 | 584.60 | 649.30 | 792.20 | 798.70 | 801.40 |
| TOA L* from nominal PLC (N) | 63.8 | 61.6 | 53.6 | 49.8 | 45.7 | 42.8 | 39.9 | 39.3 |
| TOA L* from QUASAR PLC (Q) | 51.4 | 51.4 | 39.8 | 43.2 | 32.1 | 29.1 | 26.3 | 26.7 |
| Δ TOA L* = % (Q - N)/N | -19.5% | -16.6% | -25.7% | -13.2% | -29.8% | -32.0% | -34.1% | -32.1% |
| *Date = October 5; time (UTC) = 20:29; BRF adjustment factor = 0.82.* | | | | | | | | |
| *Solar distance (A.U.) = 1.0001; solar zenith (deg) = 57.6; solar azimuth (deg) = 202.6; view zenith (deg) = 27.9; view azimuth (deg) = 283.1.* | | | | | | | | |
| Image DSL for test site (counts) | 478.50 | 486.80 | 549.80 | 584.50 | 652.60 | 792.50 | 798.20 | 803.90 |
| TOA L* from nominal PLC (N) | 63.4 | 61.3 | 53.4 | 50.1 | 46.0 | 43.8 | 39.4 | 40.6 |
| TOA L* from QUASAR PLC (Q) | 48.5 | 48.5 | 37.4 | 40.6 | 30.1 | 27.2 | 24.5 | 24.9 |
| Δ TOA L* = % (Q - N)/N | -23.4% | -20.8% | -30.0% | -19.0% | -34.6% | -37.9% | -37.9% | -38.6% |
| *Date = October 6; time (UTC) = 19:35; BRF adjustment factor = 0.80.* | | | | | | | | |
| *Solar distance (A.U.) = 0.9996; solar zenith (deg) = 55.8; solar azimuth (deg) = 186.7; view zenith (deg) = 40.7; view azimuth (deg) = 103.1.* | | | | | | | | |
| Image DSL for test site (counts) | 488.00 | 490.80 | 559.70 | 588.30 | 658.90 | 792.70 | 798.50 | 801.20 |
| TOA L* from nominal PLC (N) | 64.9 | 62.3 | 54.2 | 50.3 | 46.5 | 44.4 | 39.1 | 38.8 |
| TOA L* from QUASAR PLC (Q) | 56.2 | 55.9 | 41.9 | 45.7 | 32.8 | 29.3 | 25.6 | 26.0 |
| Δ TOA L* = % (Q - N)/N | -13.4% | -10.2% | -22.7% | -9.2% | -29.4% | -33.9% | -34.5% | -33.0% |
| *Date = October 8; time (UTC) = 19:26; BRF adjustment factor = 0.82.* | | | | | | | | |
| *Solar distance (A.U.) = 0.9990; solar zenith (deg) = 56.4; solar azimuth (deg) = 184.2; view zenith (deg) = 48.9; view azimuth (deg) = 103.1.* | | | | | | | | |
| Image DSL for test site (counts) | 550.00 | 555.40 | 630.40 | 659.40 | 721.00 | 794.70 | 799.60 | 802.30 |
| TOA L* from nominal PLC (N) | 73.5 | 71.1 | 61.7 | 57.1 | 51.6 | 48.6 | 42.0 | 41.3 |
| TOA L* from QUASAR PLC (Q) | 61.8 | 61.4 | 45.2 | 49.6 | 34.8 | 30.9 | 26.3 | 26.6 |
| Δ TOA L* = % (Q - N)/N | -15.9% | -13.7% | -26.7% | -13.1% | -32.6% | -36.4% | -37.3% | -35.6% |

[a] UTC = coordinated universal time; AU = astronomical units; RHO = surface reflectance; DSL = digital signal level; BRF = bidirectional reflectance factor; PLC = post-launch calibration; TOA = top of atmosphere.

DSL units are image counts; radiances L* units are W/(m$^2$ sr μm); irradiances units are W/(m$^2$ μm); gain units are counts/radiance.

Newell County test site latitude = 50d 18m 20s; longitude = -111d 37m 32s; elevation = 750 m.

Ozone content (cm-atm) = 0.319; water vapour content (g/cm$^2$) = 1.35.

For comparison and validation purposes, average surface reflectances from atmospherically-corrected *casi* data are compared to GER3700-based surface reflectances obtained by convolution of the average GER spectrum for the 100-meter by 100-meter ground validation site with the relative spectral response profile for the relevant satellite sensor spectral band. The agreement between the *casi*-based surface reflectances averaged over the 7-km by 7-km test site and those from the GER3700 for the ground validation site is within 10 percent in spectral band cases except VGT band B0 and SeaWiFS bands 1 and 2 (Figure 2). The agreement between *casi*-based surface reflectances restricted to pixels for the ground validation site and the GER3700-based surface reflectances for the ground validation site is within 3 percent for all spectral band cases except VGT band B0, SeaWiFS bands 1 and 2, and TM band 1. The discrepancies for lower reflectances may be due to inadequate spatial sampling of the rangeland surface with the GER3700 or reduced sensitivity in the *casi* sensor at shorter wavelengths. In general, the results are reasonable given the completely independent data and methods involved.

Table 3. TM and HRV radiometric calibrations based on the NCRA test site for October 1998 [a].

| *Date* *Otober 4, 1998* | *Landsat-5 TM* | *Landsat-5 TM* | *Landsat-5 TM* | *Landsat-5 TM* | *SPOT-2 HRV* | *SPOT-2 HRV* | *SPOT-2 HRV* |
|---|---|---|---|---|---|---|---|
| Spectral band | 1 | 2 | 3 | 4 | 1 | 2 | 3 |
| Central wavelength (µm) | 0.4863 | 0.5706 | 0.6607 | 0.8382 | 0.549 | 0.653 | 0.84 |
| Integrated bandpass (µm) | 0.0610 | 0.0763 | 0.0657 | 0.1206 | 0.0879 | 0.0644 | 0.1005 |
| Exo-atmospheric solar irradiance | 1955.5 | 1826.9 | 1545 | 1042.8 | 1802.4 | 1534.6 | 1009.2 |
| Time (UTC) | 17:56 | 17:56 | 17:56 | 17:56 | 18:36 | 18:36 | 18:36 |
| Solar distance (A.U.) | 1.0004 | 1.0004 | 1.0004 | 1.0004 | 1.0004 | 1.0004 | 1.0004 |
| Solar zenith angle (degrees) | 57.3 | 57.3 | 57.3 | 57.3 | 55.4 | 55.4 | 55.4 |
| Solar azimuth angle (degrees) | 156.3 | 156.3 | 156.3 | 156.3 | 168.09 | 168.09 | 168.09 |
| Satellite zenith angle (degrees) | 1.8 | 1.8 | 1.8 | 1.8 | 3.31 | 3.31 | 3.31 |
| Satellite azimuth angle (degrees) | 102.9 | 102.9 | 102.9 | 102.9 | 283.7 | 283.7 | 283.7 |
| Rayleigh optical depth | 0.1517 | 0.0790 | 0.0430 | 0.0168 | 0.0927 | 0.0455 | 0.0166 |
| Aerosol optical depth | 0.0575 | 0.0481 | 0.0404 | 0.0300 | 0.5020 | 0.0411 | 0.0300 |
| Test site RHO from QUASAR (TQ) | 6.2 | 8.1 | 9.8 | 16.8 | 7.7 | 9.6 | 16.8 |
| Val site RHO from GER3700 (G) | 6.8 | 8.8 | 10.4 | 18.5 | 8.3 | 10.3 | 18.5 |
| Δ RHO = % (TQ - G)/G | -9.2% | -7.6% | -6.2% | -9.1% | -7.6% | -6.7% | -9.1% |
| Val site RHO from QUASAR (VQ) | 6.5 | 8.6 | 10.1 | 18.2 | 8.1 | 10.0 | 18.2 |
| Δ RHO = % (VQ - G)/G | -4.6% | -2.5% | -2.6% | -1.6% | -2.3% | -2.9% | -1.6% |
| BRF adjustment factor | 1 | 1 | 1 | 1 | 1 | 1 | 1 |
| Image DSL for test site (counts) | 68.12 | 27.80 | 40.92 | 39.98 | 36.03 | 35.42 | 41.83 |
| Nominal PLC gain coefficient | 1.6599 | 0.8510 | 1.2411 | 1.2277 | 0.859 | 1.008 | 1.178 |
| Nominal PLC offset coefficient | 2.523 | 2.417 | 1.452 | 1.854 | 0 | 0 | 0 |
| TOA L* from nominal PLC (N) | 39.5 | 29.8 | 31.8 | 31.1 | 41.9 | 35.1 | 35.5 |
| TOA L* from QUASAR PLC (Q) | 37.9 | 31.3 | 28.8 | 28.6 | 33.9 | 29.7 | 30.1 |
| Δ TOA L* = % (Q - N)/N | -4.1% | 4.9% | -9.6% | -8.1% | -19.2% | -15.5% | -15.2% |

[a] UTC = coordinated universal time; AU = astronomical units; RHO = surface reflectance; DSL = digital signal level;
BRF = bidirectional reflectance factor; PLC = post-launch calibration; TOA = top of atmosphere.
DSL units are image counts; radiances L* units are W/(m$^2$ sr µm); irradiances units are W/(m$^2$ µm); gain units are counts/radiance.
Newell County test site latitude = 50d 18m 20s; longitude = -111d 37m 32s; elevation = 750 m.
Ozone content (cm-atm) = 0.319; water vapour content (g/cm$^2$) = 1.35.

The key QUASAR results are the TOA radiance comparisons (Tables 1 to 3). Differences are defined as (QUASAR – nominal) / nominal, in percent. Results for October 4, the *casi* data acquisition day, are shown in Figure 3. The general pattern with exceptions is that QUASAR-based TOA radiance estimates are lower than the nominal TOA radiances. The differences are –11.6 percent for AVHRR, +13.7 to -5.7 to percent for VGT, -13.2 to –34.1 percent for SeaWiFS, +4.9 to -9.6 to percent for TM, and -15.2 to –19.2 percent for HRV. QUASAR results for other days close to the *casi* data acquisition day are shown in Figure 4 together with the results for October 4. The three additional SeaWiFS cases on subsequent days (October 5, 6, and 8) also yield TOA radiances significantly lower than nominal values (differences of –9.2 to –38.6 percent). As noted with respect to the SeaWiFS results for the August 1998 campaign, SeaWiFS image acquisition geometries have close to orthogonal relative azimuths and bi-directional reflectance effects are not expected to be the main cause of these mismatches, which remain unexplained. Compared to the results for October 4, the TOA radiance comparison for AVHRR on October 5 is similar, whereas VGT TOA radiances for October 3 are a better match with nominal values. If the SeaWiFS points are excluded from Figures 3 and 4, the QUASAR results are comparable to those found previously for the NCRA test site (Figure 1).

## 8. CONCLUDING REMARKS

New QUASAR monitoring results have been generated for NOAA-14 AVHRR, OrbView-2 SeaWiFS, SPOT-4 VGT, Landsat-5 TM, and SPOT-2 HRV based on a hyperspectral data acquisition campaign at the Newell County rangeland test site in Alberta in October 1998. New results have also been obtained for SeaWiFS based on a data acquisition campaign at

Figure 2. Surface reflectance comparisons for the NCRA test site on October 4, 1998 for NOAA-14 AVHRR spectral band 1, SPOT-4 VGT spectral bands B0, B2, B3, OrbView-2 SeaWiFS spectral bands 1-8, Landsat-5 TM spectral bands 1-4, and SPOT-2 HRV spectral bands 1-3. The ± 2 percent error bars represent standard deviations typical of the data sets. The diagonal line is the unity slope line.

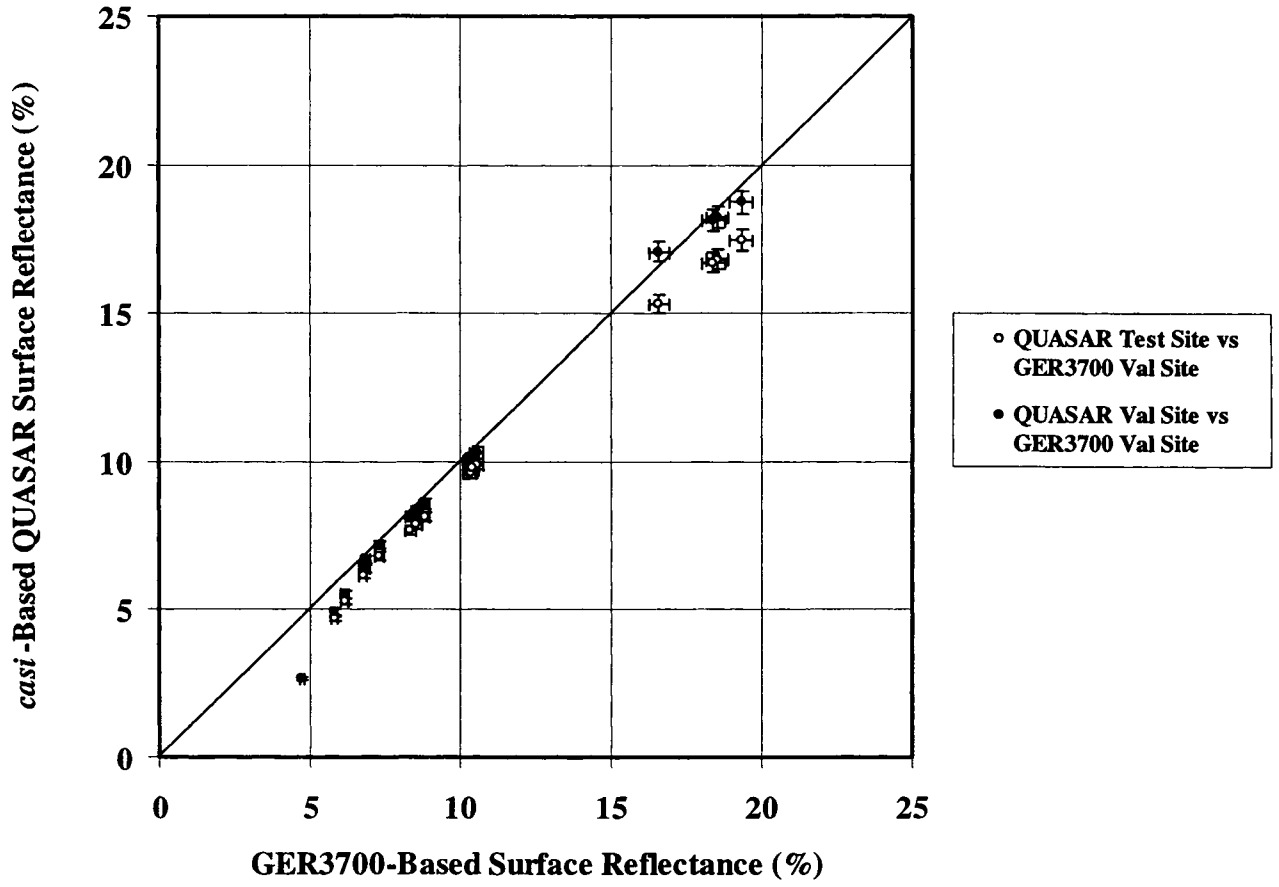


the Alberta site in August 1998. The main results consist of casi-based TOA radiance predictions and their percentage difference comparisons with satellite image-based TOA radiances determined independently using nominal post-launch calibration coefficients.

The main conclusions drawn from the new QUASAR results presented in this paper are as follows.

1. Surface reflectances obtained for the NCRA validation site from *casi*-based QUASAR spectra and GER3700-based spectra agree to within 3 percent for all spectral band cases except VGT band B0, SeaWiFS bands 1 and 2, and TM band 1.
2. For satellite data acquired on the *casi* flight day at the NCRA test site (October 4, 1998), QUASAR calibration results:
   - match within uncertainties the nominal post-launch calibration results for Landsat-5 TM bands 1 and 2 and SPOT-4 VGT band B0;
   - are within double the uncertainties compared to nominal post-launch calibration results for NOAA-14 AVHRR band 1 and Landsat-5 TM bands 3 and 4;
   - predict significantly lower TOA radiances compared to nominal post-launch calibration results for all other cases.

Figure 3. Comparison of top-of-atmosphere (TOA) radiance results for the NCRA test site for October 4, 1998 (Tables 1 to 3) for NOAA-14 AVHRR (spectral band 1), SPOT-4 VGT (spectral bands B0, B2, B3), OrbView-2 SeaWiFS (spectral bands 1-8), Landsat-5 TM (spectral bands 1-4), and SPOT-2 HRV (spectral bands 1-3). The error bars represent ± 6 percent uncertainty levels. The diagonal line is the unity slope line.

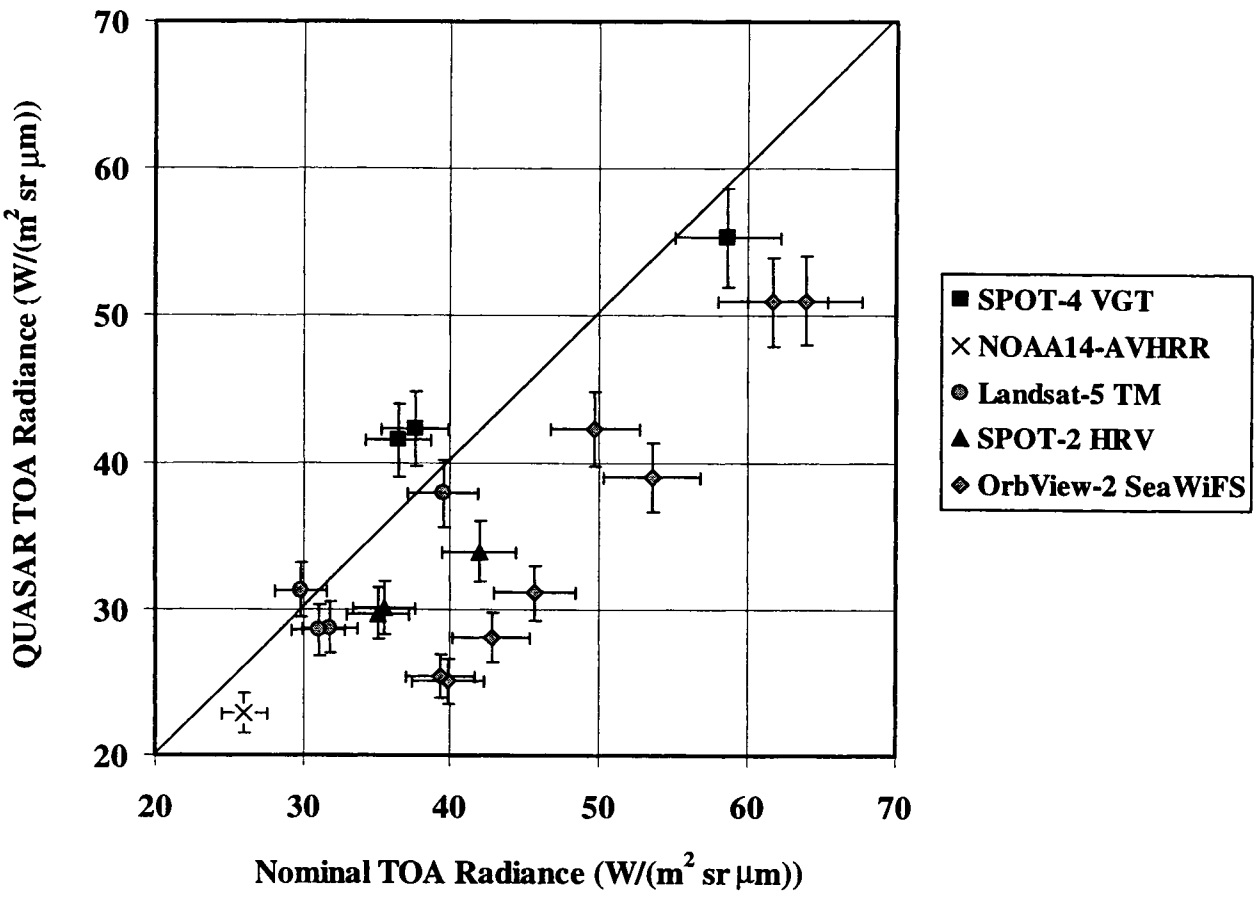


3. Temporal extensions of QUASAR data sets to days near to the *casi* data acquisition day yield:
   - reasonable results for NOAA-14 AVHRR and SPOT-4 VGT;
   - significantly lower TOA radiances compared to the nominal post-launch calibration results for OrbView-2 SeaWiFS.
4. Unlike the results for the RVPN test site, there is a systematic offset between QUASAR calibrations and nominal post-launch calibrations for all SeaWiFS cases examined for the NCRA test site (August 1998 and October 1998 campaigns). Given the overall trend in the QUASAR results for all satellite sensor cases examined to date, an investigation of potential problems with SeaDAS calibration processing (at the NASA Goddard Space Flight Center ) is warranted for the NCRA cases.
5. The pronounced, systematic offsets between QUASAR calibrations and nominal post-launch calibrations found in earlier results for the SPOT sensor cases are much less pronounced for QUASAR results for the October NCRA campaign.
6. QUASAR monitoring results for the RVPN and NCRA test sites are similar in general character and continued study of the NCRA test site as a potential test site for vicarious calibration is warranted.
7. An intercomparison of the QUASAR monitoring method with respect to independent vicarious calibration techniques remains to be done.

Figure 4. Comparison of top-of-atmosphere (TOA) radiance results for the NCRA test site for October 3-8, 1998 (Tables 1 and 2) for NOAA-14 AVHRR (spectral band 1), SPOT-4 VGT (spectral bands B0, B2, B3), OrbView-2 SeaWiFS (spectral bands 1-8), Landsat-5 TM (spectral bands 1-4), and SPOT-2 HRV (spectral bands 1-3). The error bars represent ± 6 percent uncertainty levels. The diagonal line is the unity slope line.

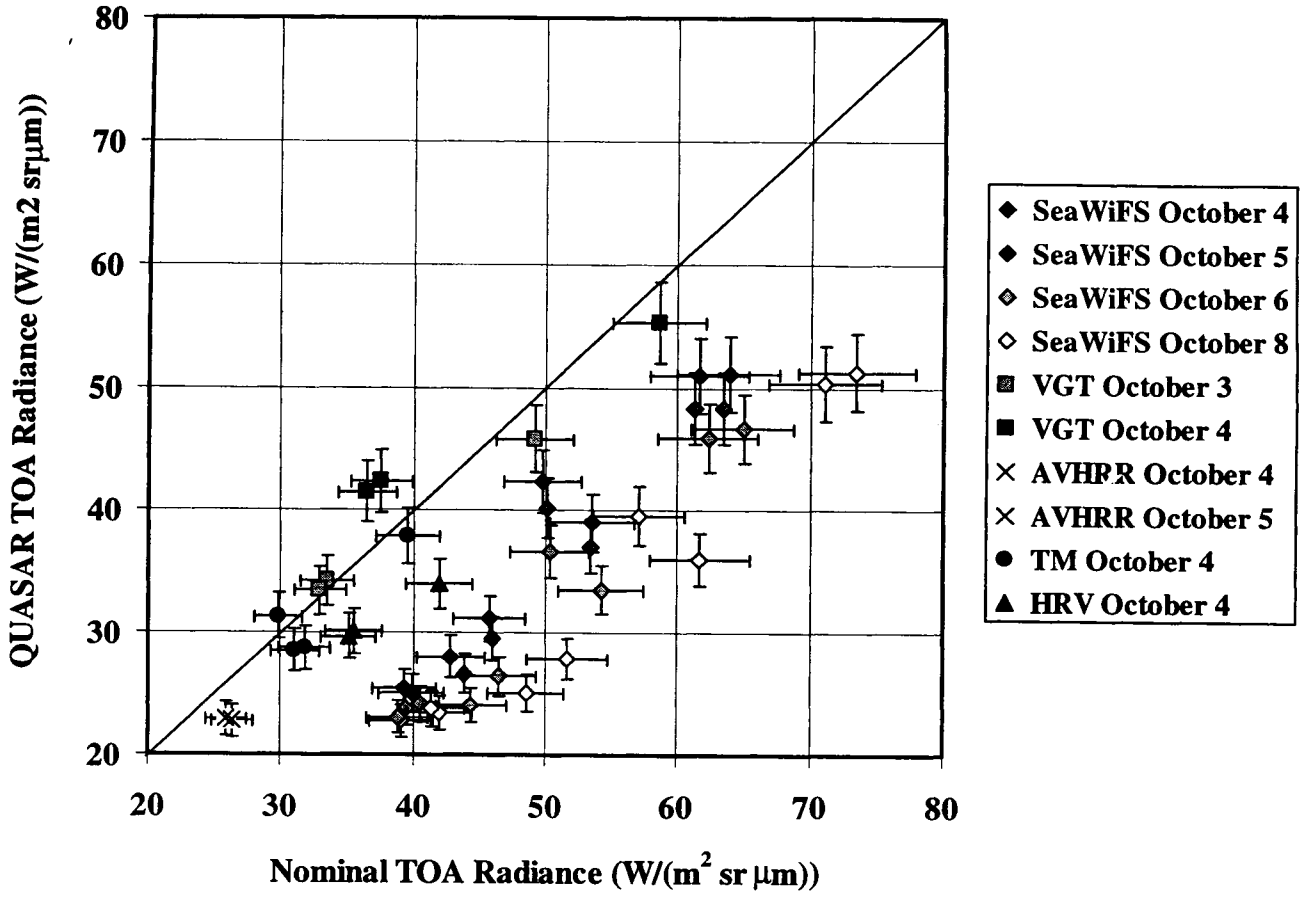


Future activities currently planned include QUASAR monitoring tests for post-launch Landsat-7 Enhanced Thematic Mapper Plus (ETM+) and EOS Terra sensor cases, additional radiometric uniformity studies of the RVPN and NCRA test sites, and a full radiometric error analysis of the QUASAR method. There is also a definite need for further work on the bi-directional reflectance characteristics of optical sensor calibration test sites. With careful refinements in these areas, the QUASAR methodology has the potential to become a generalized approach to the vicarious calibration of multiple Earth observation sensors using hyperspectral data sets.

## ACKNOWLEDGEMENTS

The authors gratefully acknowledge the technical assistance of Julie Lefebvre (MacDonald Dettwiler and Associates) with respect to ISDAS processing issues, Karen S. Baith (NASA Goddard Space Flight Center) with respect to SeaDAS processing, and Marie-Christine Laubies and Frédérique Meunier (Centre national d'études spatiales (CNES)) with respect to VGT specifications.

## REFERENCES


1. P.M. Teillet, G. Fedosejevs, R.P. Gauthier, N.T. O'Neill, K.J. Thome, S.F. Biggar, H. Ripley, and A. Meygret, "A Generalized Approach to the Vicarious Calibration of Multiple Earth Observation Sensors Using Hyperspectral Data", *Remote Sensing of Environment*, in review, 1999a.

2. P.M. Teillet, G. Fedosejevs, R.P. Gauthier, N.T. O'Neill, K.J. Thome, S.F. Biggar, H. Ripley, and A. Meygret, "Radiometric Calibration of OrbView-2 SeaWiFS and SPOT-4 Vegetation Using Airborne Hyperspectral Data", *Proceedings of the Fourth International Airborne Remote Sensing Conference and Exhibition and the Twenty-First Canadian Symposium on Remote Sensing*, Ottawa, Ontario, in press, 1999b.

3. K. Staenz, T. Szeredi, and J. Schwarz, "ISDAS – A System for Processing / Analyzing Hyperspectral Data", *Canadian Journal of Remote Sensing*, **24(2):** 99-113, 1998.

4. K. Staenz, and D.J. Williams, "Retrieval of Surface Reflectance from Hyperspectral Data Using a Look-up Table Approach", *Canadian Journal of Remote Sensing*, **23(4):** 354-368, 1997.

5. K.P. Scott, K.J. Thome, and M.R. Brownlee, "Evaluation of the Railroad Valley Playa for Use in Vicarious Calibration", *Proceedings of SPIE Conference 2818*, Denver, Colorado, 1996.

6. M. Bergeron, N.T. O'Neill, A. Royer, and P.M. Teillet, "Development of a Spectral Error Model for Surface Bidirectional Reflectance Factor (BRF) Retrieval", *Canadian Journal of Remote Sensing*, **24(2):** 128-132, 1998.

7. P.M. Teillet, G. Fedosejevs, and R.P. Gauthier, "Operational Radiometric Calibration of Broadscale Satellite Sensors Using Hyperspectral Airborne Remote Sensing of Prairie Rangeland: First Trials", *Metrologia*, **35:**639-641, 1998a.

8. P.M. Teillet, G. Fedosejevs, R.P. Gauthier, and R.A. Schowengerdt, "Uniformity Characterization of Land Test Sites Used for Radiometric Calibration of Earth Observation Sensors", *Proceedings of the Twentieth Canadian Symposium on Remote Sensing*, Calgary, Alberta, pp. 1-4, 1998b.

9. E.F. Vermote and Y.J. Kaufman, "Absolute Calibration of AVHRR Visible and Near-Infrared Channels Using Ocean and Cloud Views", *International Journal of Remote Sensing*, Calgary, **16(13):** 2317-2340, 1998b.

10. G. Fu, K.S. Baith, and C.R. McClain, "SeaDAS: The SeaWiFS Data Analysis System", *Proceedings of the 4th Pacific Ocean Remote Sensing Conference*, Qingdao, China, pp. 73-77, 1998.